E6-2010-86

G. G. Bunatian*, V. G. Nikolenko, A. B. Popov

THE USAGE OF ELECTRON BEAM TO PRODUCE RADIO ISOTOPES THROUGH THE URANIUM FISSION BY γ-RAYS AND NEUTRONS

*E-mail: bunat@cv.jinr.dubna.ru

Бунатян Г. Г., Николенко В. Г., Попов А. Б. Е6-2010-86
Использование потока электронов для производства радиоизотопов посредством деления урана γ-излучением и нейтронами

Рассматривается получение требуемых радиоизотопов посредством фотоделения ^{238}U тормозным излучением, которое порождается в конверторе исходным потоком электронов линейного ускорителя. Также исследуется образование радиоизотопов при делении ^{238}U нейтронами, которые возникают в образце урана, облучаемом этим тормозным излучением. Рассчитан выход наиболее широко применяемого в ядерной медицине изотопа ^{99}Mo. Сопоставляется получение радиоизотопов путем деления ^{238}U, исследованное в настоящей работе, с получением радиоизотопов посредством фотонейтронных ядерных реакций. Рассмотрена угроза отравления плутонием облучаемого уранового образца из-за захвата нейтронов ^{238}U. Проведенные исследования убеждают нас в том, что использование фотонейтронных ядерных реакций для производства радиоизотопов является предпочтительным по сравнению с делением ^{238}U γ-излучением и нейтронами. Использование электронных пучков современных ускорителей электронов позволяет осуществить оба метода.

Работа выполнена в Лаборатории нейтронной физики им. И. М. Франка ОИЯИ.

Сообщение Объединенного института ядерных исследований. Дубна, 2010

Bunatian G. G., Nikolenko V. G., Popov A. B. E6-2010-86
The Usage of Electron Beam to Produce Radio Isotopes through the Uranium Fission by γ-Rays and Neutrons

We treat the production of desirable radio isotopes due to the ^{238}U photo-fission by the bremsstrahlung induced in converter by an initial electron beam provided by a linear electron accelerator. We consider as well the radio isotope production through the ^{238}U fission by the neutrons that stem in the ^{238}U sample irradiated by that bremsstrahlung. The yield of the most applicable radio isotope ^{99}Mo is calculated. We correlate the findings acquired in the work presented with those obtained by treating the nuclear photo-neutron reaction. Menace of the plutonium contamination of an irradiated uranium sample because of the neutron capture by ^{238}U is considered. As we get convinced, the photo-neutron production of radio isotopes proves to be more practicable than the production by the uranium photo- and neutron-fission, both methods are certain to be brought into action due to usage of the electron beam provided by modern linear accelerators.

The investigation has been performed at the Frank Laboratory of Neutron Physics, JINR.

Communication of the Joint Institute for Nuclear Research. Dubna, 2010

1. INTRODUCTION. AGENDA OF ISOTOPE PRODUCTION BY ELECTRON BEAM

Nowadays, there exists the unwaning anxiety around the world about the shortage of nuclear isotopes used in numerous fields of the medicine and life science [1–6]. One of the most important artificially made radionuclide is the molybdenum-99, ^{99}Mo, because of the world-wide use of its daughter metastable nuclide technetium-99, ^{99}Tc, in nuclear medicine. Currently, the predominant process of ^{99}Mo production utilizes the $^{235}\mathrm{U}\,(n, fission)\,^{99}\mathrm{Mo}$ reaction and requires nuclear high-flux reactors and highly-enriched-uranium (HEU) samples. Recent years many a profound work [6–10] have been considering and highlighting the manifold flaws inherent in this method. Alternative new facilities and processes are needed. To construct anew a dedicated modern reactor is far more, about ten times, expensive than a modern multi-MW linear electron accelerator, e-linac. Moreover, timely reactors are very difficult to build due to manifold regulatory and political concerns as well. The time to build a new e-linac and commission the respective isotope production can reasonably be no more than ~ 3 years, which is unrealistic for a reactor case. In the issue, the global problem of a safe and reliable supply of radio isotopes for use in the life science is believed to be solved with e-linacs, not high-flux reactors, no matter whether HEU or LEU is utilized to prepare the samples irradiated by neutrons in reactor.

As the reactor-based isotope production is to give place to the e-linac-driven production, we are to treat the electron beam, with an energy distribution $\rho_e(E_e)$ and a current density $J_e(t)$[A/cm^2] (generally time-dependent), which produces in converter (see Fig. 1) the bremsstrahlung with a flux density

$$J_\gamma(E_\gamma) = \frac{\mathcal{N}_\gamma(E_\gamma)}{\mathrm{s}\cdot\mathrm{cm}^2\cdot\mathrm{MeV}}, \qquad (1.1)$$

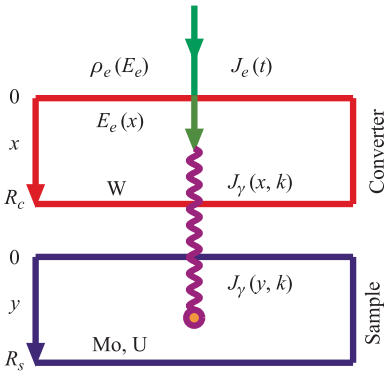

Fig. 1. The setup scheme

expressed in terms of the photon number $\mathcal{N}_\gamma(E_\gamma)$ with the energy $E_\gamma = |\mathbf{k}| = k$, per 1 cm^2, 1 s, 1 MeV. In turn, by irradiating an appropriate sample, this bremsstrahlung induces the manifold photo-nuclear reactions, which can serve to obtain various desirable isotopes.

First and foremost, as observed in Refs. [11–14], the well-known process

$$\gamma + A(Z,N) \Longrightarrow A'(Z,N-1) + n \tag{1.2}$$

is quite practicable to produce a needful isotope $A(Z,N-1)$, which was explicated to the full in the previous work [15].

In Sec. 2, we consider the ^{99}Mo yield due to the ^{238}U fission directly by the bremsstrahlung (1.1). The neutron production in an uranium sample irradiated by this γ-flux (1.1) is discussed in Sec. 3. These neutrons, in turn, induce the ^{238}U fission which results in an additional ^{99}Mo production, as described in Sec. 4. The total outcome of ^{99}Mo amount and activity is evaluated in Sec. 5. In Sec. 6, the occurrence of the harmful ^{239}Pu isotope, accompanying the ^{99}Mo production, is considered. In conclusion, in Sec. 7, we correlate concisely once again the various practicable methods, currently at our disposal, to produce needful isotopes.

2. THE ^{238}U PHOTO-FISSION TO PRODUCE RADIO ISOTOPES

Now, the point is to treat the uranium photo-fission

$$\gamma + {}^{238}\mathrm{U} \Longrightarrow \textit{fission fragments} + \nu_\gamma \textit{ fission neutrons}, \tag{2.1}$$

induced by the γ-flux (1.1), with subsequent recovery of a desirable isotope from the blend of photo-fission fragments. Apparently, one recognizes at once this design mimicks the well-known routine method to yield isotopes by irradiating highly- or low-enriched uranium targets on the high-flux research and test reactors [3–7]. Actually, alike in the work [15], the key point is that the process (2.1) can successively run only provided the relation

$$E_\gamma, E_e \gtrsim E_{\mathrm{GR}} \sim 10 \text{ MeV} \tag{2.2}$$

between the energies E_e, E_γ and the energy E_{GR} of giant nuclear resonance [16] holds, as one realizes from Fig. 2, where the ^{238}U photo-fission cross section $\sigma_{\gamma F}$ [17] is presented simultaneously with the γ-flux density $J_\gamma(E_\gamma)$ converted from the electron beam, with various energies E_e, in the tungsten converter with the size R_W (see Fig. 1), most preferable at a given energy E_e. Thus, only the electrons and photons with energies (2.2) provide the process (2.1), as a matter of fact. As in the work [15], we restrict also our ensuing consideration by the electron energies

$$E_e \leqslant 100 \text{ MeV} \tag{2.3}$$

as well. Mostly, the findings are further discussed for the actually practicable energy $E_e = 50$ MeV. In the previous work [15], we acquired the quantity $J_\gamma(E_\gamma)$ (1.1). The bremsstrahlung flux at final edge of a tungsten converter with a given size R_W was fined

$$J_{\gamma\,W}(k, R_W, Z_W, \rho_W, E_e^b, E_e^u, \Delta_e, t) = J_e(t)\mathcal{N}_W \times$$
$$\times \int\limits_{E_e^b}^{E_e^u} \mathrm{d}E \rho_e(E) \int\limits_0^{R_W} \mathrm{d}x \frac{\mathrm{d}\sigma_b(k, E_e(x,E), Z_W)}{\mathrm{d}k} \cdot \exp\left(-\frac{R_W - x}{l_W(Z_W, \mathcal{N}_W, k, \rho_W)}\right). \tag{2.4}$$

Here $\dfrac{\mathrm{d}\sigma_b(k, E_e(x,E), Z_W)}{\mathrm{d}k}$ is the cross section of bremsstrahlung of an electron with the energy $E_e(x,E)$ at a distance x from the starting edge of converter, see Refs. [18–22]. The last exponent in (2.4) describes the γ-flux decrease in converter passing, determined by the γ-ray absorption length $l_W(k)$ in tungsten [18–20, 23]. Given the electron initial energy $E_e(0) = E$, the dependence $E_e(x,E)$ was obtained in Ref. [15] in terms of the tungsten converter characteristics. In the expression (2.4), the number $\mathcal{N}_W$ of scattering atoms of converter in 1 cm^3 is

$$\mathcal{N}_W = \frac{\rho_W \cdot 6.022 \cdot 10^{23}}{A_W}, \tag{2.5}$$

where $\rho_W = 18.7$ g/cm^3 is the density of converter material, and $A_W = 184$ is its atomic weight. In the expression (2.4), the quantities E_e^b, E_e^u are, respectively, the bottom and upper energies of the electron distribution in beam, and Δ_e is to describe its width. The electron energy varies between the limits E_e^b, E_e^u, and

$$\rho_e(E) = \frac{1}{n} \exp\left[-((E - \bar{E})/\Delta_e)^2\right], \quad \bar{E} = \frac{E_e^b + E_e^u}{2}, \tag{2.6}$$
$$1 = \int\limits_{E_e^b}^{E_e^u} \mathrm{d}E \rho_e(E).$$

We carry out the further evaluations at

1) $\bar{E}_e = 20$ MeV, with $E_e^b = 19.5$ MeV, $E_e^u = 20.5$ MeV, $\Delta_e = 0.2$ MeV; $R_W = 0.1$ cm.

2) $\bar{E}_e = 25$ MeV, with $E_e^b = 24.5$ MeV, $E_e^u = 25.5$ MeV, $\Delta_e = 0.2$ MeV; $R_W = 0.18$ cm.

3) $\bar{E}_e = 50$ MeV, with $E_e^b = 48.5$ MeV, $E_e^u = 52.5$ MeV, $\Delta_e = 0.5$ MeV;
$R_W = 0.3$ cm. (2.7)

4) $\bar{E}_e = 100$ MeV, with $E_e^b = 95$ MeV, $E_e^u = 105$ MeV, $\Delta_e = 1.0$ MeV;
$R_W = 0.4$ cm.

The optimum values of converter size R_W, found out in the work [15], are designated for every electron energy as well. Generally speaking, the γ-flux inducing the reaction (2.1) could be produced by an initial electron beam just in the ^{238}U sample itself, without an additional W-converter expressly arranged. Yet we treat purposely the γ-flux converted in a separate W-converter just in the same way as in the previous work [15], in order to correlate immediately the ability to produce ^{99}Mo due to the reaction (2.1) with the ^{99}Mo production through the reaction (1.2).

The respective $J_{\gamma W}(k, R_W, Z_W, \rho_W, E_e^b, E_e^u, \Delta_e, t)$ values (2.4) at the starting edge of an ^{238}U sample (for time-independent J_e) are shown in Fig. 2, for given $\bar{E}_e$ (2.7) and the R_W values most efficient at respective $\bar{E}_e$ [15]. Let us recall that we do not take care of the feasible electron–photon cascade as the

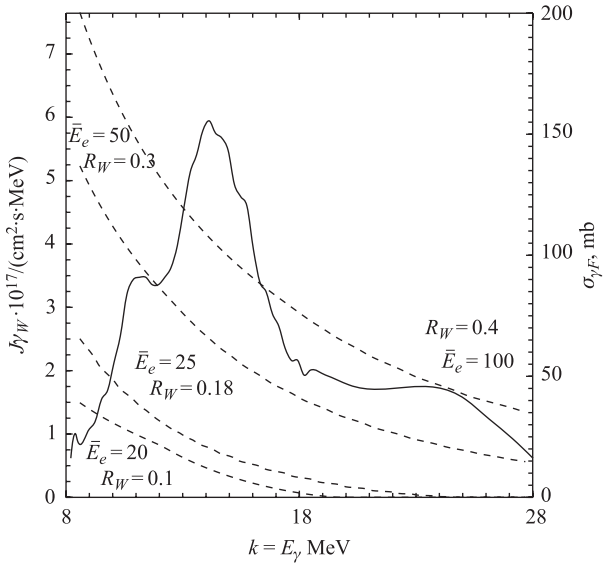

Fig. 2. The dashed curves represent the k-dependence of the γ-flux (2.4) at the final edge of converter for various $\bar{E}_e$ (MeV) (2.7) and the most preferable thicknesses R_W (cm), which are plotted alongside the respective curves. The initial electron current density $J_e = 1$ A/cm^2. The solid curve represents k-dependence of the cross section of reaction in Eq. (2.1)

particles participating therein would primarily have got energies beyond the key condition (2.2) (see Ref. [15]).

Traveling forward through the uranium sample (see Fig. 1), the γ-flux (2.4) diminishes in much the same way as in passing the W-converter, yet the uranium absorption length $l_U(k)$ comes into consideration in place of the tungsten absorption length $l_W(k)$ [23]. Upon passing a distance y from starting edge of uranium sample (see Fig. 1), the γ-flux (2.4) modifies as follows:

$$J_{\gamma\,U}(y,k,R_W,Z_W,\rho_W,Z_U,\rho_U,\bar{E}_e,t) = \\ = J_{\gamma\,W}(k,R_W,Z_W,\rho_W,\bar{E}_e,t)\exp\left[-\frac{y}{l_U(Z_U,\mathcal{N}_U,\rho_U,k)}\right]. \quad (2.8)$$

Consequently, we obtain total rate of the γ-fission process (2.1), i.e. total number of events of the ^{238}U fission, $\mathcal{N}_{\gamma F}(R_U,R_W,\bar{E}_e,t)$, induced by the photon current density (2.4) within an uranium sample, with a given size R_U, per 1 s, per 1 cm^2 of sample area,

$$\frac{\mathcal{N}_{\gamma F}(R_U,R_W,\bar{E}_e,J_e,t)}{\mathrm{d}t} = J_e(t)\cdot\mathcal{N}^0_{\gamma F}(R_U,R_W,\bar{E}_e), \quad (2.9)$$

$$\mathcal{N}^0_{\gamma F}(R_U,R_W,\bar{E}_e) = \mathcal{N}_U\cdot\mathcal{N}_W\cdot\int\limits_{E_e^b}^{E_e^u}\mathrm{d}E\rho_e(E)\times \\ \times\int\limits_0^\infty \mathrm{d}k\sigma_{\gamma F}(k,{}^{238}\mathrm{U})\left(1-\exp[-\frac{R_U}{l_U(k)}]\right)l_U(k)\times \\ \times\int\limits_0^{R_W}\mathrm{d}x\exp\left[-\frac{R_W-x}{l_W(k)}\right]\left(\frac{\mathrm{d}\sigma_b(k,E_e(x,E),W)}{\mathrm{d}k}\right), \quad (2.10)$$

where the density of uranium atoms of sample

$$\mathcal{N}_U = \frac{\rho_U\cdot 6.022\cdot 10^{23}}{A_U} \quad (2.11)$$

is given in terms of the density $\rho_U = 18.5$ g/cm^3 and the atomic weight $A_U = 238$ g. The uranium γ-fission cross section, that governs the photo-fission rate (2.9), (2.10), was carefully explored, and we utilized the $\sigma_{\gamma F}(k,\ ^{238}\mathrm{U})$ data acquired in Ref. [17]. It is to keep in view that in the expressions (2.8)–(2.10) and others hereafter, the argument $\bar{E}_e$, for the sake of conciseness, stands for

electron energy distribution, as offered in Eqs. (2.6), (2.7), with the respective $\bar{E}_e$ value.

As explicated in Introduction, our primary purpose is to calculate the yield of the ^{99}Mo isotope, which is the precursor of the today most applicable in nuclear medicine radio isotope ^{99m}Tc. Among uranium photo-fission fragments, the ^{99}Mo radio isotope constitutes $\approx 6.06\%$, in a few minutes after the fission [24,25]. Therefore, in the uranium photo-fission the rate of ^{99}Mo production is just obtained by multiplying the expression (2.10) by the factor 0.0606, so that the yield of ^{99}Mo is given by

$$\frac{\mathcal{N}_{\gamma F^{99}\mathrm{Mo}}(R_U, R_W, \bar{E}_e, J_e, t)}{\mathrm{d}t} = 0.0606 \cdot \frac{\mathcal{N}_{\gamma F}(R_U, R_W, \bar{E}_e, J_e, t)}{\mathrm{d}t}. \qquad (2.12)$$

It is here to recall the current $J_{\gamma U}(\bar{E}_e)$ (2.8), for the actual values of $(\bar{E}_e)$, was ascertained in the work [15] with the accuracy $\sim 10\%$. The accuracy of the cross section $\sigma_{\gamma F}(k,^{238}\mathrm{U})$ measurement, which rules the quantity (2.12) evaluation, was asserted to be $\sim 10\%$ as well [17]. Thus, the accuracy of evaluation of the ^{99}Mo production rate (2.12) proves to be $\sim 10\%$.

3. GENERATING THE PHOTO-NEUTRONS IN URANIUM SAMPLE

Besides the heretofore considered uranium photo-fission, we are to explore the uranium fission by neutrons, which leads to the yield of ^{99}Mo as well. The γ-flux $J_{\gamma U}$ (2.8) traveling through uranium sample produces neutrons due to the ordinary photo-nuclear reactions [16, 17]

$$\gamma + {}^{238}\mathrm{U} = n + {}^{237}\mathrm{U}, \qquad (3.1)$$

$$\gamma + {}^{238}\mathrm{U} = 2n + {}^{236}\mathrm{U}, \qquad (3.2)$$

$$\gamma + {}^{238}\mathrm{U} = 3n + {}^{235}\mathrm{U}. \qquad (3.3)$$

As well, the photo-fission reaction (2.1) is known to be accompanied by the neutrons number

$$\nu_\gamma(k) \approx 0.158\frac{k}{\mathrm{MeV}} + 1.5, \qquad (3.4)$$

where $k = E_\gamma$ (MeV) is the energy of a photon inducing ^{238}U fission [23–25]. The dependence of the giant resonance cross sections $\sigma_{\gamma rn}(k), (r = 1, 2, 3)$ of the processes (3.1)–(3.3) and the γ-fission cross section $\sigma_{\gamma F}(k)$ on the photon energy $k = E_\gamma$ was thoroughly explored, and we utilize the data from Refs. [17] in our calculation. The contribution of the $(\gamma, 3n)$ reaction (3.3) into the actual neutron spectrum is rather negligibly small in our case, so that we shall abandon it afterwards.

In the case considered, the neutrons from the photon-induced giant resonance reactions (3.1)–(3.3) consist primarily of evaporation neutrons and a small fraction of «direct» neutrons as well. The energy distribution of the single neutron evaporation in the process (3.1) can best be described by the Weisskopf statistical model [17, 26–29]

$$\frac{\mathrm{d}n^{st}_{\gamma 1n}(\epsilon, k, \mathbf{a})}{\mathrm{d}\epsilon} = \epsilon \exp\left[2\sqrt{\mathbf{a}\cdot(k - B_{1n} - \epsilon)}\right]\times \\ \times\, \Theta(k - B_{1n} - \epsilon)\cdot\Theta(\epsilon - k + B_{2n})\frac{1}{\mathcal{N}_{\gamma 1n}(k)}, \quad (3.5)$$

with the assumption that a second neutron is always emitted in a compound nuclear reaction whenever its emission is energetically possible [17, 26–28]. Here $\epsilon = E_n - m_n$ is the neutron kinetic energy, B_{1n}, B_{2n} are the $(\gamma, 1n)$, (3.1) and $(\gamma, 2n)$, (3.2) thresholds, respectively, and $\mathbf{a}$ stands for the nuclear density parameter [17, 27, 28], whereas $\mathcal{N}_{\gamma 1n}(k)$ is the normalization factor still to be determined (see further Eq. (3.9)). Dealing in our case with an ^{238}U sample, we utilize the values $B_{1n} \approx 5.97$ MeV, $B_{2n} \approx 11.27$ MeV, $\mathbf{a}(^{237}\mathrm{U}) \approx 20$ MeV^{-1}, as asserted in Ref. [17].

A discernible fraction $\chi(E_\gamma)$ of photo-absorption events is known to lead to the direct photo-neutron emission [17, 26–29], and the higher the photon energy E_γ, the higher the direct neutron fraction. As one can infer from the findings of Refs. [17, 26–29], the linear relationship

$$\chi(E_\gamma) \approx 0.02\cdot\Theta(E_\gamma - B_{1n} - 2.5)\cdot(E_\gamma - B_{1n} - 2.5)\ [\mathrm{MeV}] \quad (3.6)$$

is pertinent to estimate the fraction of direct neutron emission in the process (3.1), so as it is to say that there are no direct neutrons at $E_\gamma - B_{1n} < 2.5$ MeV, and at $E_\gamma \gtrsim E_{\mathrm{GR}}$ the evaporation neutrons constitute about 0.8 of all the neutrons produced. As was observed [17, 26–29], the direct neutron spectra from heavy deformed nuclei have peaks about $\sim 10\%$ lower than the value of $\epsilon \approx E_\gamma - B_{1n}$. Therefore, the direct neutron spectrum in the reaction (3.1) is suitable to be considered as being constant between the neutron energy values of $\epsilon = E_\gamma - B_{1n}$ and $\epsilon = \mathrm{D}(E_\gamma - B_{1n})$, with the parameter $\mathrm{D} \approx 0.3$ (see Ref. [29]), so as we assume for the direct neutron energy distribution the estimation

$$\frac{\mathrm{d}n^{d}_{\gamma 1n}(\epsilon, E_\gamma)}{\mathrm{d}\epsilon} = \frac{1}{1-\mathrm{D}}\int\limits_{\mathrm{D}}^{1}\mathrm{d}\eta\,\delta(\epsilon - \eta(E_\gamma - B_{1n})). \quad (3.7)$$

Apparently, this $\sqcap$-shaped function tends to $\delta(\epsilon - E_\gamma + B_{1n})$ when $\mathrm{D} \to 1$.

The energy distribution of all neutrons emitted in the reaction (3.1) is

$$\frac{\mathrm{d}\tilde{n}_{\gamma 1n}(\epsilon,k,a)}{\mathrm{d}\epsilon}=\frac{\mathrm{d}n^{st}_{\gamma 1n}(\epsilon,k,\mathbf{a})}{\mathrm{d}\epsilon}(1-\chi(k))+$$
$$+\chi(k)\cdot\Theta(k-B_{1n}-\epsilon)\cdot\Theta(\epsilon-k+B_{2n})\frac{\mathrm{d}n^{d}_{\gamma 1n}(\epsilon,E_\gamma)}{\mathrm{d}\epsilon}, \quad (3.8)$$

normalized so that

$$\int\limits_0^\infty \mathrm{d}\epsilon\frac{\mathrm{d}\tilde{n}_{\gamma 1n}(\epsilon,k,a)}{\mathrm{d}\epsilon}=1. \quad (3.9)$$

The spectrum of the first of two neutrons, that are emitted in the reaction (3.2) when $k=E_\gamma>B_{2n}+\epsilon$, is written likewise (3.5)

$$\frac{\mathrm{d}n^{st}_{\gamma 2n}(\epsilon,k,\mathbf{a})}{\mathrm{d}\epsilon}=\epsilon\exp\left[2\sqrt{\mathbf{a}\cdot(k-B_{1n}-\epsilon)}\right]\Theta(k-B_{2n}-\epsilon)\frac{1}{\mathcal{N}_{\gamma 2n}(k)}, \quad (3.10)$$

normalized so that

$$\int\limits_0^\infty \mathrm{d}\epsilon\frac{\mathrm{d}n^{st}_{\gamma 2n}(\epsilon,k,\mathbf{a})}{\mathrm{d}\epsilon}=1. \quad (3.11)$$

The energy distribution of the second neutron emitted in the reaction (3.2) is described as follows [27, 28]:

$$\frac{\mathrm{d}\tilde{n}^{st}_{\gamma 2n}(\epsilon,k,\mathbf{a},\tilde{\mathbf{a}})}{\mathrm{d}\epsilon}=\int\limits_0^\infty \mathrm{d}\epsilon'\epsilon'\exp\left[2\sqrt{\mathbf{a}\cdot(k-B_{1n}-\epsilon')}\right]\times$$
$$\times\,\Theta(k-B_{2n}-\epsilon-\epsilon')\frac{\mathrm{d}\tilde{n}^{st}_{\gamma 1n}(\epsilon,\epsilon',k,\tilde{\mathbf{a}})}{\mathrm{d}\epsilon}\cdot\frac{1}{\mathcal{N}'_{\gamma 2n}(k)}, \quad (3.12)$$

where

$$\frac{\mathrm{d}\tilde{n}^{st}_{\gamma 1n}(\epsilon,\epsilon',k,\tilde{\mathbf{a}})}{\mathrm{d}\epsilon}=\epsilon\cdot\exp\left[2\sqrt{\tilde{\mathbf{a}}\cdot(k-B_{2n}-\epsilon-\epsilon')}\right], \quad (3.13)$$

and the normalization factor $\mathcal{N}'_{\gamma 2n}$ is determined according to the condition

$$\int\limits_0^\infty \mathrm{d}\epsilon\frac{\mathrm{d}\tilde{n}^{st}_{\gamma 2n}(\epsilon,k,\mathbf{a},\tilde{\mathbf{a}})}{\mathrm{d}\epsilon}=1. \quad (3.14)$$

We assume the quantity $\tilde{\mathbf{a}}$ associated with the ^{236}U level density parameter is believed to be estimated by the ^{237}U level density parameter, $\tilde{\mathbf{a}}\approx\mathbf{a}\approx 20$ MeV^{-1}, cited above.

Neutron energy spectrum in the reaction (3.2) can be presumed to be pure evaporational, as the energy of emitted neutrons is in this reaction substantially smaller than in the process (3.1).

Surely, the evaporation neutrons angular distribution is just purely isotropic. Although angular distribution of direct neutrons, that constitute never more than $\approx 10\%$, is known to be not isotropic, the relations

$$m_U \gg E_\gamma = k, \quad \epsilon = E_n - m_n, \tag{3.15}$$

enable us to utilize an average isotropic distribution in our further evaluations, with an accuracy anyway not worse than $\sim 10\%$.

The energy distribution of the neutrons $\nu_\gamma(k)$ (3.4), accompanying the uranium γ-fission, is generally received (see Refs. [24, 25]) to be described by the function

$$\boldsymbol{f}_\gamma(\epsilon) = \frac{2\sqrt{\epsilon}}{\sqrt{\pi T^3}} \exp\left[-\frac{\epsilon}{T}\right], \quad T = \frac{4}{3}\ (\text{MeV}), \tag{3.16}$$

so as the mean energy of the emitted ν_γ neutrons shows up to be $\bar{\epsilon} = 2$ MeV.

Then, with allowance for Eqs. (2.4), (2.8)–(2.10), (3.5)–(3.14), the density of neutrons with the energy ϵ produced per 1 s at a distance y from the initial edge of uranium sample (see Figs. 1, 3) proves to be

$$\frac{\mathrm{d}^2 n_\gamma(\epsilon, y, t)}{\mathrm{d}t \mathrm{d}\epsilon} = J_e(t) \cdot n^0_\gamma(y, \epsilon), \tag{3.17}$$

$$\begin{aligned} n^0_\gamma(y,\epsilon) = \mathcal{N}_U \cdot \mathcal{N}_W \cdot \int\limits_{E_e^b}^{E_e^u} \rho_e(E)\mathrm{d}E \Bigg\{ \int\limits_0^\infty \mathrm{d}k \frac{\mathrm{d}n_\gamma(\epsilon,k)}{\mathrm{d}\epsilon} \exp\left[-\frac{y}{\ell_U(k)}\right] \times \\ \times \int\limits_0^{R_W} \mathrm{d}x \exp\left[-\frac{R_W - x}{\ell_W(k)}\right] \frac{\mathrm{d}\sigma_b(k, E_e(x,E), W)}{\mathrm{d}k} + \\ + \boldsymbol{f}_\gamma(\epsilon) \int\limits_0^\infty \mathrm{d}k \cdot \nu_\gamma(k)\sigma_{\gamma F}(k) \exp\left[-\frac{y}{\ell_U(k)}\right] \times \\ \times \int\limits_0^{R_W} \mathrm{d}x \exp\left[-\frac{R_W - x}{\ell_W(k)}\right] \frac{\mathrm{d}\sigma_b(k, E_e(x,E), W)}{\mathrm{d}k} \Bigg\}, \end{aligned} \tag{3.18}$$

$$\begin{aligned} \frac{\mathrm{d}n_\gamma(\epsilon,k)}{\mathrm{d}\epsilon} = \sigma_{\gamma 1n}(k) \frac{\mathrm{d}\tilde{n}_{\gamma 1n}(\epsilon,k,a)}{\mathrm{d}\epsilon} + \\ + \sigma_{\gamma 2n}(k) \left\{ \frac{\mathrm{d}n^{st}_{\gamma 2n}(\epsilon,k,\mathbf{a})}{\mathrm{d}\epsilon} + \frac{\mathrm{d}\tilde{n}^{st}_{\gamma 2n}(\epsilon,k,\mathbf{a},\tilde{\mathbf{a}})}{\mathrm{d}\epsilon} \right\}. \end{aligned} \tag{3.19}$$

Upon integrating the expression (3.17) over emitted neutron energy ϵ, we would arrive, due to the proper normalization conditions (3.9), (3.11), (3.14), at the total rate of neutron production in terms of the cross sections $\sigma_{\gamma 1n}(k)$, $\sigma_{\gamma 2n}(k)$, $\sigma_{\gamma F}(k)$ of the reactions (3.1), (3.2), (2.1). Evidently, in evaluating heretofore any integrals over neutron energy ϵ, one must keep in mind that the statistical description of neutron photo-production is valid only for a large enough absorbed photon energy $E_\gamma = k$, so that at least the relation

$$E_\gamma - B_{1n,2n} \gtrsim \frac{1}{\mathbf{a}} \sim 0.05 \text{ MeV} \tag{3.20}$$

has to hold, recalling the aforesaid value $\mathbf{a} \approx 20 \text{ MeV}^{-1}$. Obviously, the cross sections $\sigma_{\gamma 1n}(k)$, $\sigma_{\gamma 2n}(k)$, $\sigma_{\gamma F}(k)$ are negligible otherwise. As realized, the expressions (3.17)–(3.19) describe production of the first neutron generation in an uranium sample due to γ-flux irradiating.

With reliance in the above-explicated consideration, we become plainly convinced that the energies of the emitted neutrons are primarily distributed in a vicinity of a mean value $\bar{\epsilon}$, which constitutes a few MeV's [17, 26–29]. At such energies ϵ, the respective cross sections (see further Eq. (4.1)) to describe the interactions of neutrons with ^{238}U nuclei are found to be about a few barns [30–32]. This observation will be of actual use in the evaluations what follow, in Sec. 4.

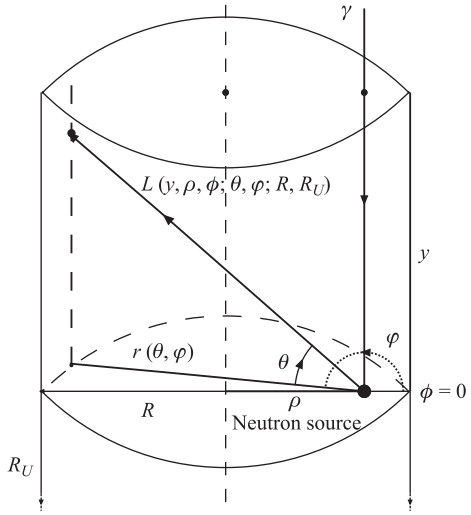

Fig. 3. The outline of neutrons stem at the point (y, ρ, ϕ) and their subsequent spread in the direction (θ, φ) within uranium sample, until leaving it, on covering the distance $L(y, \rho, \phi; \theta, \varphi; R_U, R)$. R_U, R are the length and radius of the cylinder-shaped sample

For the sake of definiteness, we shall hereafter consider a cylindrical uranium sample with the radius R and the length $H = R_U$, chosen properly afterwards.

Let

$$n(\epsilon, t; 0) = \frac{\mathrm{d}^2 n_\gamma(\epsilon, y, \rho, \phi, t)}{\mathrm{d}\epsilon \mathrm{d}t} \tag{3.21}$$

be density of the first generation neutrons with the energy ϵ produced at a point with cylindrical coordinates y, ρ, ϕ, chosen to be an origin. Figure 3 outlines the path of neutrons, originating at the point (y, ρ, ϕ), through the sample, until leaving it. Then, assuming the uranium sample be homogeneous, this quantity $n(\epsilon, t; 0)$ (3.21) does not apparently depend on (ρ, ϕ), and is directly determined by Eqs. (3.17), (3.18). This quantity can be considered as intensity of a source, placed at an original point (y, ρ, ϕ), of sphere symmetrically distributed neutrons with a given energy ϵ. Intensity of the neutron flux from this source in a direction (θ, φ), at a distance L from the origin (y, ρ, ϕ) reads as

$$n(\epsilon, t; \theta, \varphi, L) = \frac{\mathrm{d}^2 n_\gamma(\epsilon, y, \rho, \phi, t; \theta, \varphi, L)}{\mathrm{d}\epsilon \mathrm{d}t}. \tag{3.22}$$

This quantity is determined by the standard equation

$$\frac{\mathrm{d}n(\epsilon, t; \theta, \varphi, L)}{\mathrm{d}L} = \mathcal{N}_U \cdot \sigma_{t\,n}(\epsilon) \cdot n(\epsilon, t; \theta, \varphi, L), \tag{3.23}$$

with the ordinary boundary condition

$$n(\epsilon, t; \theta, \varphi, L = 0) = \frac{n(\epsilon, t; 0)}{4\pi} \sin(\theta) \mathrm{d}\theta \mathrm{d}\varphi, \tag{3.24}$$

that is the neutron flux in the direction (θ, φ) with the energy ϵ, just at the neutron source. The quantity $\sigma_{t\,n}(\epsilon)$ in Eq. (3.23) stands to describe all the alteration of the quantity (3.22) due to neutron interactions in uranium sample. All the knowledge about $\sigma_{tn}(\epsilon)$ we are in need of is acquired from Refs. [30–34]. It suits here to write $\sigma_{tn}(\epsilon) = -\sigma_{\mathrm{dec}}(\epsilon) + \sigma_{\mathrm{inc}}(\epsilon)$, where $\sigma_{\mathrm{dec}}(\epsilon)$ and $\sigma_{\mathrm{inc}}(\epsilon)$ serve to describe decrease and increase of the neutron flux (3.22), respectively. Thus, at a distance L from the origin we have got

$$n(\epsilon, t; \theta, \varphi, L) = \frac{n(\epsilon, t; 0)}{4\pi} \sin(\theta) \mathrm{d}\theta \mathrm{d}\varphi \cdot \exp\left[L \cdot \mathcal{N}_U \cdot \sigma_{t\,n}(\epsilon)\right], \tag{3.25}$$

that is the number of neutrons within the solid angle $\sin\theta \mathrm{d}\theta \mathrm{d}\varphi$ that have passed the distance L from the source where they have been produced. Thus, we have considered the firstly generated neutron flux and its subsequent feasible distortion in traveling through a sample.

4. ISOTOPE PRODUCTION DUE TO THE ^{238}U FISSION BY NEUTRONS

Interacting with uranium, the first generation neutrons induce manifold nuclear reactions which results in formation of different nuclei. Let each of these reactions, with a respective cross section $\sigma_{n\mathbf{S}}(\epsilon)$, be specified with a tag $\mathbf{S}$. Surely, we can write

$$\sigma_{tn}(\epsilon) = \sum_{\mathbf{S}} \sigma_{n\mathbf{S}}(\epsilon). \tag{4.1}$$

The rate of reaction on a unite of path L is determined through the quantities (3.22)–(3.25)

$$\frac{\mathrm{d}}{\mathrm{d}L} \cdot \frac{\mathrm{d}^2\mathcal{N}_{n\mathbf{S}}(\epsilon, y, \rho, \phi, t; \theta, \varphi, L)}{\mathrm{d}\epsilon \mathrm{d}t} = \frac{\mathrm{d}^2 n_\gamma(\epsilon, y, \rho, \phi, t; \theta, \varphi, L)}{\mathrm{d}\epsilon \mathrm{d}t} \mathcal{N}_U \cdot \sigma_{n\mathbf{S}}(\epsilon). \tag{4.2}$$

Then, the whole rate of a reaction $\mathbf{S}$, induced along all the distance L by neutrons (3.25) that originate at the point (y, ρ, ϕ) and then spread in the direction (θ, φ), reads as follows:

$$\frac{\mathrm{d}^2\mathcal{N}_{n\,\mathbf{S}}(\epsilon, y, \rho, \phi, t; \theta, \varphi, L)}{\mathrm{d}\epsilon \mathrm{d}t} = \frac{n(\epsilon, t, 0)}{4\pi} \sin(\theta) \mathrm{d}\theta \mathrm{d}\varphi \times \\ \times \sigma_{n\mathbf{S}}(\epsilon) \frac{\exp\left[\mathcal{N}_U \cdot \sigma_{tn}(\epsilon) \cdot L\right] - 1}{\sigma_{tn}(\epsilon)}. \tag{4.3}$$

Traveling in a direction defined by angles (θ, φ), (see Fig. 3) these neutrons (3.25), on covering the distance $L(y, \rho, \phi; \theta, \varphi; R, R_U)$, reach the surface of uranium sample and leave it. The angle $\theta(y, \rho, \varphi; R, R_U)$ at which neutrons come across the sample surface and the distance $L(y, \rho, \phi; \theta, \varphi; R, R_U)$ covered thereby are determined by the shape and size of a sample (see Fig. 3). Upon integrating the expression (4.3) over the neutron energy ϵ, over the appropriate angles (θ, φ), and also over all the sample volume (that is over the variables y, ρ and multiplying by the factor 2π with setting $\phi = 0$ in the expressions (3.21), (3.22) and in the covered distance $L(y, \rho, \phi; \theta, \varphi; R, R_U)$) we arrive at the total rate of a reaction $\mathbf{S}$

$$\frac{\mathrm{d}\mathcal{N}_{n\,\mathbf{S}}(t)}{\mathrm{d}t} = \int_0^\infty \mathrm{d}\epsilon \frac{\sigma_{n\mathbf{S}}(\epsilon)}{\sigma_{tn}(\epsilon)} \int_0^{R_U} \mathrm{d}y \int_0^R \rho \mathrm{d}\rho \cdot \frac{\mathrm{d}^2 n_\gamma(\epsilon, y, \rho, 0, t)}{\mathrm{d}\epsilon \mathrm{d}t} \times \\ \times \int_0^\pi \mathrm{d}\varphi \int_{-\pi/2}^{\pi/2} \mathrm{d}\theta \sin\theta \left(\exp\left[\mathcal{N}_U \cdot \sigma_{tn}(\epsilon) \cdot L(y, \rho, 0; \theta, \varphi; R, R_U)\right] - 1\right). \tag{4.4}$$

Assumed the uranium sample be cylinder-shaped, with the length $H = R_U$ and the radius R (see Fig. 3), the last integral over θ in the expression (4.4)

proves to be plainly presented in the form

$$I(\rho,\varphi)=\int\limits_{-\pi/2}^{\pi/2}\mathrm{d}\theta\sin\theta(\exp\left[\mathcal{N}_U\cdot\sigma_{tn}(\epsilon)\cdot L(y,\rho,0;\theta,\phi;R,R_U)\right]-1)=$$

$$=\int\limits_{0}^{\Theta_m(\rho,\varphi)}\mathrm{d}\theta\sin\theta(\exp\left[\mathcal{N}_U\cdot\sigma_{tn}(\epsilon)\cdot L_t(\rho,\varphi)\right]-1)+$$

$$+\int\limits_{0}^{\Theta'_m(\rho,\varphi)}\mathrm{d}\theta\sin\theta(\exp\left[\mathcal{N}_U\cdot\sigma_{tn}(\epsilon)\cdot L_t(\rho,\varphi)\right]-1)+$$

$$+\int\limits_{\Theta_m(\rho,\varphi)}^{\pi/2}\mathrm{d}\theta\sin\theta(\exp\left[\mathcal{N}_U\cdot\sigma_{tn}(\epsilon)\cdot\tilde{L}_t(\rho,\varphi)\right]-1)+$$

$$+\int\limits_{\Theta'_m(\rho,\varphi)}^{\pi/2}\mathrm{d}\theta\sin\theta(\exp\left[\mathcal{N}_U\sigma_{tn}(\epsilon)\tilde{L}'_t(\rho,\varphi)\right]-1). \quad (4.5)$$

Here the quantities are introduced

$$\begin{aligned} &L_t=\frac{r(\rho,\varphi)}{\cos\theta},\quad \tilde{L}_t=\frac{R_U-y}{\sin\theta},\quad \tilde{L}'_t=\frac{y}{\sin\theta},\\ &\Theta_m=\arctan\frac{R_U-y}{r(\rho,\varphi)},\quad \Theta'_m=\arctan\frac{y}{r(\rho,\varphi)}, \end{aligned} \quad (4.6)$$

with

$$r(\rho,\varphi)=-\rho\cos\varphi+\sqrt{R^2-\rho^2\sin^2(\varphi)}. \quad (4.7)$$

Let us recall that the expressions (4.2), (4.3) stand to describe the rate of a reaction **S**, induced just by those first generation neutrons (3.22), (3.25) that stem at the original point (y,ρ,ϕ) due to reactions (2.1), (3.1), (3.2), and then pass the distance $L(y,\rho,\phi;\theta,\varphi;R,R_U)$ in the direction (θ,φ) until leaving uranium sample (see Fig. 3). The current work does not concern the feasible production of the second, third, etc., neutron generations by these original neutrons of the first generation. Such an approach holds when the quantity $\mathcal{N}_U\cdot\sigma_{tn}\cdot L(y,\rho,\phi;\theta,\varphi;R,R_U)$ turns out to be small enough, so that the original neutron flux, in passing the distance $L(y,\rho,\phi;\theta,\varphi;R,R_U)$, does not undergo any tangible modification, and, consequently, there is no discernible production of succeeding neutrons, which in turn could induce various reactions in sample. Thus, when $\mathcal{N}_U\cdot\sigma_{tn}\cdot L(y,\rho,\phi;\theta,\varphi;R,R_U)\ll 1$, all the reactions **S** can be

treated as induced only by the original photo-neutrons, which stem immediately from in the processes (3.1), (3.2), (2.1).

Now, we are to estimate the mean distance $\bar{L}$ covered by neutrons until leaving the uranium sample. In much the same way as the expressions (4.5)–(4.7) were acquired, this results in

$$\bar{L} = \frac{1}{\pi R^2 R_U} \int\limits_0^{R_U} \mathrm{d}y \int\limits_0^{\pi} \mathrm{d}\varphi \int\limits_0^{R} \rho \mathrm{d}\rho \left(r(\rho,\varphi) \left[\int\limits_0^{\Theta_m} \mathrm{d}\theta \tan\theta + \right.\right.$$
$$\left.\left. + \int\limits_0^{\Theta'_m} \mathrm{d}\theta \tan\theta \right] + (R_U - y) \int\limits_{\Theta_m}^{\pi/2} \mathrm{d}\theta + y \int\limits_{\Theta_m}^{\pi/2} \mathrm{d}\theta \right) =$$
$$= \frac{4R}{3\pi} \left(\ln \frac{R^2 + R_U^2}{R^2} - 1 \right) + \frac{R_U \pi}{4} - \left(\frac{R_U}{2} - \frac{R^2}{2R_U} \right) \arctan \frac{8R_U}{3\pi R}. \quad (4.8)$$

In the actual evaluations what follow, we deal with the values $R \approx 0.5$ cm, $R_U \lesssim 10$ cm, so that there is rather plain estimation

$$\bar{L} \lesssim 1 \text{ cm}. \quad (4.9)$$

Let us recall, the values of cross sections $\sigma_{tn}(\epsilon)$ (4.1) are understood to be a few barns at the neutron energy ϵ being actually a few MeV's [17,26–33], as was already discussed above, in Sec. 3. Then, with allowance for the $\mathcal{N}_U$ value (2.11), the powers of exponents in the expressions (4.4), (4.5) are estimated to be anyway small enough

$$\mathcal{N}_U \cdot \sigma_{tn}(\bar{\epsilon}) \cdot \bar{L} \sim 0.1, \quad (4.10)$$

so as those exponents can be expanded into a power series, with retaining the first-order terms only, which implies that all the processes nonlinear in the cross sections $\sigma_{n\mathbf{S}}$ are left out of consideration.

Then, the rate of reaction (4.4) reduces, with a sufficient accuracy $\sim 10\%$, to

$$\frac{\mathrm{d}\mathcal{N}_{n\,\mathbf{S}}(R_U, R_W, \bar{E}_e, J_e, t)}{\mathrm{d}t} \approx$$
$$\approx \mathcal{N}_U \int\limits_0^{\infty} \mathrm{d}\epsilon \sigma_{n\mathbf{S}}(\epsilon) \int\limits_0^{R_U} \mathrm{d}y \int\limits_0^{R} \rho \mathrm{d}\rho \frac{\mathrm{d}^2 n_\gamma(\epsilon, y, \rho, 0, t)}{\mathrm{d}\epsilon \mathrm{d}t} \int\limits_0^{\pi} \mathrm{d}\varphi \times$$
$$\times \{ r \ln[(r^2 + (R_U - y)^2)^{1/2} \cdot (r^2 + y^2)^{1/2} / r^2] + \frac{R_U \pi}{2} -$$
$$- (R_U - y) \arctan \frac{R_U - y}{r} - y \arctan \frac{y}{r} \}, \quad (4.11)$$

with the function r given by Eq. (4.7). Here, in writing arguments of the function $\mathcal{N}_{n\,\mathbf{S}}(R_U, R_W, \bar{E}_e, J_e, t)$, the initial electron energy $\bar{E}_e$ and current J_e, and the sizes of converter R_W and sample R_U are purposely recalled. As realized, the current calculation is reduced, with an accuracy $\sim 10\%$, as we allow for only those reactions which are induced immediately by the first generation photoneutrons (3.1), (3.2), (2.1), whereas the original flux of these neutrons themselves is suggested suffering no discernible perturbations to be taken into consideration, in passing through the considered uranium sample.

If anything, still following reducing this expression (4.11) proves to be relevant. The dependence of the expression within curly brackets in Eq. (4.11) on variable y, especially as being under a $\ln$ and $\arctan$ sign, is far more smooth than the exponential dependence $\exp\left[-y/\ell_U(k)\right]$ on y of the function (3.18). Then, the expression in curly brackets can be replaced by its value averaged over the sample length R_U. Next, the functions $r(\rho,\varphi), r^2(\rho,\varphi)$, when standing under a $\ln$ and $\arctan$ sign, can be replaced by their mean values over sample area. Then, the integrations over variables y, ρ, φ were performed directly in Eq. (4.11), and it would be written in the explicit plain form

$$\frac{\mathrm{d}\mathcal{N}_{n\,\mathbf{S}}(R_U, R_W, \bar{E}_e, J_e, t)}{\mathrm{d}t} \approx J_e(t) \cdot \mathcal{N}^0_{n\,\mathbf{S}}(R_U, R_W, \bar{E}_e), \tag{4.12}$$

$$\begin{aligned}
\mathcal{N}^0_{n\,\mathbf{S}}(R_U, R_W, \bar{E}_e) = \mathcal{N}_U \cdot \mathcal{N}_U \cdot \mathcal{N}_W \cdot \int\limits_{E_e^b}^{E_e^u} \mathrm{d}E \rho_e(E) \int\limits_0^\infty \mathrm{d}\epsilon \sigma_{n\mathbf{S}}(\epsilon) \times \\
\times \left\{ \int\limits_0^\infty \mathrm{d}k \frac{\mathrm{d}n_\gamma(\epsilon,k)}{\mathrm{d}\epsilon} \left(1 - \exp\left[-\frac{R_U}{\ell_U(k)}\right]\right) \ell_U(k) \times \right. \\
\times \int\limits_0^{R_W} \mathrm{d}x \exp\left[-\frac{R_W - x}{\ell_W(k)}\right] \frac{\mathrm{d}\sigma_b(k, E_e(x,E), W)}{\mathrm{d}k} + \\
+ \boldsymbol{f}_\gamma(\epsilon) \int\limits_0^\infty \mathrm{d}k \nu_\gamma(k) \sigma_{\gamma F}(k) \left(1 - \exp\left[-\frac{R_U}{\ell_U(k)}\right]\right) \ell_U(k) \times \\
\left. \times \int\limits_0^{R_W} \mathrm{d}x \exp\left[-\frac{R_W - x}{\ell_W(k)}\right] \frac{\mathrm{d}\sigma_b(k, E_e(x,E), W)}{\mathrm{d}k} \right\} \times \\
\times \left\{ \frac{4R^3}{3} \left(\ln \frac{R_U^2 + R^2}{R^2} - 1 \right) + \frac{R_U \pi}{4} \pi R^2 - \pi R^2 \left(\frac{R_U}{2} - \frac{R^2}{2R_U} \right) \arctan \frac{8R_U}{3\pi R} \right\},
\end{aligned} \tag{4.13}$$

with the function $\dfrac{\mathrm{d}n_\gamma(\epsilon,k)}{\mathrm{d}\epsilon}$ determined by Eq. (3.19).

Now we are to treat the uranium fission by the first generation neutrons produced in uranium sample through its γ irradiating. Then, the expressions (4.2)–(4.4), (4.11)–(4.13), with the tag $\mathbf{S} = F$, and the ^{238}U n-fission cross section $\sigma_{n\mathbf{S}}(\epsilon) = \sigma_{nF}(\epsilon)$, describe the rate of the reaction

$$n + {}^{238}\mathrm{U} \Rightarrow \textit{ fission fragments} + \nu_n \textit{ neutrons}. \tag{4.14}$$

The quantity $\sigma_{nF}(\epsilon, {}^{238}\mathrm{U})$ is well measured, and we utilize its values acquired in Refs. [31–33].

5. THE RADIO ISOTOPE YIELD IN IRRADIATING ^{238}U SAMPLE

It is to repeat here, the aim of the current calculation is not to treat the neutrons issue, yet the yield of a desired isotope through the ^{238}U fission by γ-rays and the first generation neutrons produced immediately by these γ-rays inside a sample. Our primary purpose is now to acquire the isotope ^{99}Mo production due to the reaction (4.14). Alike in the photo-fission (2.1), the isotope ^{99}Mo constitutes $\approx 6\%$ in the blend of fission fragments, in a few minutes after the fission [24, 25]. Then, the yield of ^{99}Mo, $\mathcal{N}_{n\,F\,Mo}(R_U, R_W, \bar{E}_e, J_e, t)$, is given by Eqs. (4.11), (4.13) multiplied by the factor ≈ 0.06

$$\frac{\mathrm{d}\mathcal{N}_{n\,F\,Mo}(R_U, R_W, \bar{E}_e, J_e, t)}{\mathrm{d}t} \approx 0.06 \frac{\mathrm{d}\mathcal{N}_{n\,F}(R_U, R_W, \bar{E}_e, J_e, t)}{\mathrm{d}t}. \tag{5.1}$$

The sum of Eqs. (2.12) and (5.1),

$$\frac{\mathrm{d}\mathcal{N}_{\mathrm{sum}\,F\,Mo}(R_U, R_W, \bar{E}_e, J_e, t)}{\mathrm{d}t} = \\ = \frac{\mathrm{d}\mathcal{N}_{\gamma\,F\,Mo}(R_U, R_W, \bar{E}_e, J_e, t)}{\mathrm{d}t} + \frac{\mathrm{d}\mathcal{N}_{n\,F\,Mo}(R_U, R_W, \bar{E}_e, J_e, t)}{\mathrm{d}t}, \tag{5.2}$$

gives the total yield of ^{99}Mo isotope in the uranium sample with a given size R_U, per 1 s, per 1 cm^2 of sample area, due to an electron beam with the current density $J_e(t)$ and the electron energy $\bar{E}_e$ converted in the γ-flux (2.4) by the tungsten converter with a given size R_W.

It is here to emphasize that any assumptions used in calculating the ^{99}Mo production through the ^{238}U fission by neutrons (5.1) were thoroughly examined and justified, so as the sufficient accurateness $\sim 20\%$ is believed to be provided, to all appearance. All the more that the ^{99}Mo production by the ^{238}U neutron-fission (5.1) itself constitutes $\sim 10\%$ to the ^{238}U photo-fission production of ^{99}Mo (2.12), what is seen from the numerical results presented hereafter.

The expressions (2.12), (5.1), (5.2) represent sources to produce the ^{99}Mo isotope, that decays with the lifetime $\tau = \tau_{^{99}\mathrm{Mo}} \approx 96$ h, so that the number of decays per 1 s reads ordinarily

$$\frac{\mathcal{N}_{i\,F\,Mo}(t;\tau)}{\tau}, \quad i = \mathrm{sum}, \gamma, n.$$

The isotope ^{99}Mo itself undergoes irradiation by the same γ-flux (2.8) as ^{238}U does. Then, the photo-nuclear reaction

$$\gamma + {}^{99}\mathrm{Mo} \rightarrow {}^{98}\mathrm{Mo} + n \tag{5.3}$$

results in depletion of the generated isotope ^{99}Mo,

$$-\frac{\mathcal{N}_{i\,F\,Mo}(t;\tau)}{\mathcal{N}_U} \cdot \frac{\mathrm{d}\mathcal{N}_{i\,F\,Mo}(R_U, R_W, \bar{E}_e, J_e, t)}{\mathrm{d}t}, \tag{5.4}$$

which was acquired in the previous work [15]. Though this correction (5.4) is to be allowed for, its impact on the isotope production is very small, rather negligible, at the values of T_e, J_e treated hereafter.

Then, amenably to the common equation

$$\frac{\mathrm{d}\mathcal{N}_{i\,F\,Mo}(R_U, R_W, \bar{E}_e, J_e, t;\tau)}{\mathrm{d}t} = \frac{\mathrm{d}\mathcal{N}_{i\,F\,Mo}(R_U, R_W, \bar{E}_e, J_e, t)}{\mathrm{d}t} - \\ - \frac{\mathcal{N}_{i\,F\,Mo}(t;\tau)}{\tau} - \frac{\mathcal{N}_{i\,F\,Mo}(t;\tau)}{\mathcal{N}_U} \cdot \frac{\mathrm{d}\mathcal{N}_{i\,F\,Mo}(R_U, R_W, \bar{E}_e, t)}{\mathrm{d}t}, \tag{5.5}$$

the ^{99}Mo amount, per 1 cm^2 area of the sample, worked up during an exposition time T_e, is given as

$$\mathcal{N}_{i\,F\,Mo}(R_U, R_W, \bar{E}_e, J_e, T_e;\tau) = \\ = \int\limits_0^{T_e} \mathrm{d}t \frac{\mathrm{d}\mathcal{N}_{i\,F\,Mo}(R_U, R_W, \bar{E}_e, J_e, t)}{\mathrm{d}t} \exp\left[t/\tilde{\tau}\right] \cdot \exp\left[-T_e/\tilde{\tau}\right], \tag{5.6}$$

$$\frac{1}{\tilde{\tau}} = \frac{1}{\tau} + \frac{\mathcal{N}_{i\,F\,Mo}(t;\tau)}{\mathcal{N}_U} \cdot \frac{\mathrm{d}\mathcal{N}_{i\,F\,Mo}(R_U, R_W, \bar{E}_e, J_e, t)}{\mathrm{d}t}. \tag{5.7}$$

For a time-independent initial electron current J_e in main Eqs. (4.11), (4.12), the expression (5.6) reduces to

$$\mathcal{N}_{i\,F\,Mo}(R_U, R_W, \bar{E}_e, J_e, T_e;\tau) = J_e \mathcal{N}^0_{i\,F\,Mo}(R_U, R_W, \bar{E}_e)\tilde{\tau}(1 - \exp\left[-T_e/\tilde{\tau}\right]). \tag{5.8}$$

When $T_e \ll \tau$, this gets simplified, giving just

$$\mathcal{N}_{i\,F\,Mo}(R_U, R_W, \bar{E}_e, J_e, T_e; \tau) = J_e \cdot \mathcal{N}^0_{i\,F\,Mo}(R_U, R_W, \bar{E}_e) \cdot T_e. \qquad (5.9)$$

It is to designate that we have been using, all over the carried out calculations, just the lifetime τ, yet not the so-called half-decay period $T_{1/2} = \tau \ln 2$.

The total amount of the ^{99}Mo isotope produced in a whole uranium sample with 1 cm^2 area, during exposition time T_e is

$$\mathcal{M}_{i\,F\,Mo}(\mathrm{g}) = \frac{\mathcal{N}_{i\,F\,Mo}(R_U, R_W, \bar{E}_e, J_e, T_e; \tau) \cdot 99(\mathrm{g})}{6.022{\cdot}10^{23}}, \quad i = \mathrm{sum}, \gamma, n, \; (5.10)$$

where the quantities $\mathcal{N}_{\mathrm{sum}\,F\,Mo}$, $\mathcal{N}_{\gamma\,F\,Mo}$, $\mathcal{N}_{n\,F\,Mo}$ are given by Eqs. (5.6), (5.8), (5.9).

As is generally accepted (see, for instance, Refs. [11–15]), the radio isotope production is described in terms of the so-called specific activity yield $Y[\mathrm{Bq}/(\mathrm{h} \cdot \mu\mathrm{A} \cdot \mathrm{mg}\, A(Z,N))]$ in Bq per 1 h of exposition time, per 1 μA of the initial electron current J_e, and per 1 mg of the isotope $A(Z,N)$ in the sample, which serves to produce the desirable isotope $A'(Z',N')$, the ^{99}Mo isotope in the case considered. Just according to its definition, this characteristic Y for the ^{99}Mo production due to the ^{238}U fission is natural to be defined as

$$Y_{i\,F\,Mo}(\mathrm{Bq}) = \frac{\mathcal{N}_{i\,F\,Mo}(R_U, R_W, \bar{E}_e, J_e, T_e; \tau)}{R_U(\mathrm{cm}) \cdot \rho_U(\mathrm{mg/cm^3}) \cdot \tau(\mathrm{s}) \cdot T_e(\mathrm{h}) \cdot J_e(\mu\mathrm{A})}, \qquad (5.11)$$

provided the uranium sample is 1 cm^2 area. It is also of use to consider the total yield of activity produced due to an initial electron current J_e inside the whole uranium sample, with 1 cm^2 area and a given thickness R_U, during an exposition time T_e

$$\mathcal{Y}_{i\,F\,Mo}(\mathrm{Bq}) = \frac{\mathcal{N}_{i\,F\,Mo}(R_U, R_W, \bar{E}_e, J_e, T_e; \tau)}{\tau(\mathrm{s})}. \qquad (5.12)$$

Now we turn to discussing the quantities $\mathcal{M}, Y, \mathcal{Y}$ evaluated at the different initial electron energies $\bar{E}_e$ (2.7), corresponding tungsten converter sizes R_W, uranium sample sizes R_U, and at various exposition time T_e.

For the purposes proclaimed in Introduction, it is here wise and expedient to discuss these results along with the findings of the work [15]. Therefore, the values of $\mathcal{M}, Y, \mathcal{Y}$ evaluated in the current work are presented in the following figures and tables side by side with their respective values from Ref. [15]. As one infer from observing Tables 1–3, the ^{99}Mo production in the reaction $^{100}\mathrm{Mo}(\gamma, n)^{99}\mathrm{Mo}$, which was explored in Ref. [15], is far more profitable than the ^{99}Mo recovery from the ^{238}U fission fragments, acquired in the current work. In fact, the values of $\mathcal{M}_{\mathrm{sum}\,F\,Mo}, \mathcal{Y}_{\mathrm{sum}\,F\,Mo}$ are about twenty times as small as the $\mathcal{M}_{\gamma\,Mo}$ and $\mathcal{Y}_{\gamma\,Mo}$ values, whereas the values of $Y_{\mathrm{sum}\,F\,Mo}$ show up

Table 1. The amounts $\mathcal{M}[\mathbf{mg}\cdot 10^{-2}]$ of ^{99}Mo produced in ^{100}Mo and ^{238}U samples (5.10), with $R_S = 2$ cm , ($S =$ Mo, U) and 1 cm^2 area, by the electron current with $\bar{E}_e$ [MeV] and $J_e = 1$ A/cm^2, during 1 h exposition. The second string represents $\mathcal{M}$ obtained in the reaction ^{100}Mo$(\gamma, n)^{99}$Mo, and the third one describes the ^{99}Mo production in the U photo-fission, whereas the forth row stands for $\mathcal{M}$ value received in ^{238}U fission by neutrons, which stem within U sample during its γ irradiating. The values in the last row are sums of the respective values in the third and the forth ones

$\bar{E}_e$	20.0	25.0	50.0	100.0
$\mathcal{M}_{\gamma\, Mo}$[a]	161.0	332.0	951.0	1593.0
$\mathcal{M}_{\gamma\, F\, Mo}$	7.3	14.2	42.0	72.4
$\mathcal{M}_{n\, F\, Mo}$	0.83	1.55	4.1	6.9
$\mathcal{M}_{\mathrm{sum}\, F\, Mo}$	8.31	15.75	46.1	79.3

[a]The data from Ref. [15].

Table 2. The yield $Y[\frac{\mathbf{kBq}}{\mathbf{h}\cdot\mu\mathbf{A}\cdot\mathbf{mg}^{100}\mathbf{Mo\ or\ }^{238}\mathbf{U}}]$ of ^{99}Mo specific activity produced in ^{100}Mo and ^{238}U samples (5.11) with $R_S = 2$ cm ($S =$ Mo, U) and 1 cm^2 area, caused by the electron current with $\bar{E}_e$ [MeV] and $J_e = 1$ A/cm^2, during 1 h exposition. The second string presents $Y[\frac{\mathbf{kBq}}{\mathbf{h}\cdot\mu\mathbf{A}\cdot\mathbf{mg}^{100}\mathbf{Mo}}]$ of ^{99}Mo obtained in the reaction ^{100}Mo$(\gamma, n)^{99}$Mo, and the third one gives the quantity $Y[\frac{\mathbf{kBq}}{\mathbf{h}\cdot\mu\mathbf{A}\cdot\mathbf{mg}^{238}\mathbf{U}}]$ of ^{99}Mo produced in the ^{238}U photo-fission, whereas the forth one gives the ^{99}Mo activity $Y[\frac{\mathbf{kBq}}{\mathbf{h}\cdot\mu\mathbf{A}\cdot\mathbf{mg}^{238}\mathbf{U}}]$ received in the ^{238}U fission by neutrons, which stem within U sample during its γ irradiating. The values in the last row are sums of the respective values in the third and the forth ones

$\bar{E}_e$	20.0	25.0	50.0	100.0
$Y_{\gamma\, Mo}$[a]	1.49	2.97	8.55	14.37
$Y_{\gamma\, F\, Mo}$	0.034	0.067	0.19	0.34
$Y_{n\, F\, Mo}$	0.004	0.0072	0.019	0.032
$Y_{\mathrm{sum}\, F\, Mo}$	0.038	0.074	0.209	0.372

[a]The data from Ref. [15].

even to be forty times as small as $Y_{\gamma\, Mo}$, at any given energies of electron beam. As seen from Tables 1–3, the energy growth from $\bar{E}_e = 20$ MeV to $\bar{E}_e = 50$ MeV results in about six times increase of ^{99}Mo yield, whereas the ^{99}Mo yield at $\bar{E}_e = 100$ MeV is at best only about twice that at $\bar{E}_e = 50$ MeV. So, enhancing the initial electron energy above ≈ 50 MeV is rather of small value, as was already ascertained in the work [15]. Next, let us note, the quantities $\mathcal{M}_{n\, F\, Mo}$, $Y_{n\, F\, Mo}$, $\mathcal{Y}_{n\, F\, Mo}$ constitute only about 10% to $\mathcal{M}_{\gamma\, F\, Mo}$, $Y_{\gamma\, F\, Mo}$, $\mathcal{Y}_{\gamma\, F\, Mo}$, so as the primary part of ^{99}Mo production is anyway due to the imme-

Table 3. The yield $\mathcal{Y}$[kBq$\cdot 10^{10}$] of ^{99}Mo total activity produced in ^{100}Mo and ^{238}U (5.12) samples with $R_S = 2$ cm ($S =$ Mo, U) and 1 cm^2 area, due to the electron current with $\bar{E}_e$[MeV] and $J_e = 1$ A/cm^2, during 1 h exposition. The second string presents $\mathcal{Y}$ obtained in the reaction ^{100}Mo$(\gamma, n)^{99}$Mo, and the third one describes ^{99}Mo production in the U photo-fission, whereas the forth row stands for $\mathcal{Y}$ received in the ^{238}U fission by neutrons, which stem within U sample during its γ irradiating. The values in the last row are sums of the respective values in the third and the forth ones

$\bar{E}_e$	20.0	25.0	50.0	100.0
$\mathcal{Y}_{\gamma\, Mo}$[a]	2.9	5.86	16.87	28.17
$\mathcal{Y}_{\gamma\, F\, Mo}$	0.13	0.25	0.73	1.275
$\mathcal{Y}_{n\, F\, Mo}$	0.015	0.027	0.075	0.13
$\mathcal{Y}_{\mathrm{sum}\, F\, Mo}$	0.145	0.277	0.805	1.405

[a]The data from Ref. [15].

diate uranium γ fission, yet not due to the uranium fission by neutrons stemming in irradiating the considered uranium sample by a given γ-flux. These findings validate the transformation of the expressions (4.4), (4.3) to (4.11).

Surely, if the natural molybdenum sample, containing only $\approx 10\%$ of the ^{100}Mo isotope, were utilized in the reaction $^{\mathrm{nat}}$Mo$(\gamma, n)^{99}$Mo instead of the pure ^{100}Mo sample, the yield of ^{99}Mo isotope would be ten times smaller than given in Tables. Then, the ^{99}Mo isotope yield $\mathcal{M}_{\gamma\, F\, Mo}, Y_{\gamma\, F\, Mo}, \mathcal{Y}_{\gamma\, F\, Mo}$ in the photo-neutron reaction, as explored in [15], would be only about twice as much as the ^{99}Mo yield in the uranium photo-fission, $\mathcal{M}_{\mathrm{sum}\, F\, Mo}, Y_{\mathrm{sum}\, F\, Mo}, \mathcal{Y}_{\mathrm{sum}\, F\, Mo}$. The ^{99}Mo production in the photo-neutron reaction on a natural molybdenum $^{\mathrm{nat}}$Mo sample shows up anyway to be no more than two-three times as much as the ^{99}Mo yield in the uranium photo-fission. Thus, in this case, advantage of the ^{99}Mo photo-neutron production over the ^{99}Mo production in the uranium photo-fission could not be said to be substantial. In the figures what follow, we shall directly display just the results obtained in utilizing the natural $^{\mathrm{nat}}$Mo sample [15].

For practical application, we are to acquire how do the quantities $\mathcal{M}_{\mathrm{sum}\, F\, Mo}$, $Y_{\mathrm{sum}\, F\, Mo}$, $\mathcal{Y}_{\mathrm{sum}\, F\, Mo}$ vary with the length R_U of uranium sample. The dependence of these quantities on R_U, as displayed in Figs. 4–6, is substantially nonlinear at $R_U \gtrsim 3$ cm, alike the dependence $\mathcal{M}_{\gamma\, Mo}(R_{Mo}), Y_{\gamma\, Mo}(R_{Mo})$, $\mathcal{Y}_{\gamma\, Mo}(R_{Mo})$, acquired in the work [15]. The functions $\mathcal{M}_{\mathrm{sum}\, F\, Mo}(R_U)$, $\mathcal{Y}_{\mathrm{sum}\, F\, Mo}(R_U)$ get apparent saturation, and the function $Y_{\mathrm{sum}\, F\, Mo}(R_U)$ gets discernible decrease. Thus, there sees no reason to make the length R_U greater than 2–3 cm, just alike the length R_{Mo} of molybdenum sample in producing ^{99}Mo in the photo-neutron reaction $^{\mathrm{nat,100}}$Mo$(\gamma, n)^{99}$Mo, which was acquired in Ref. [15].

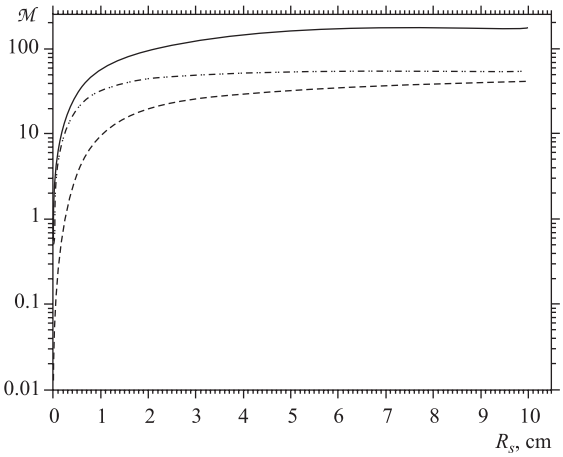

Fig. 4. The amounts $\mathcal{M}(\text{mg} \cdot 10^{-2})$ of ^{99}Mo and ^{239}Pu isotopes, produced within natural molybdenum and uranium samples, with the size $R_S\,(S = Mo, U)$ and area 1 cm^2, by the electron current with $\bar{E}_e = 50$ MeV and $J_e = 1$ A/cm^2, during 1 h. The solid line presents the R_{Mo}-dependence of the quantity $\mathcal{M}_{\gamma\,Mo}(R_{Mo})$ obtained in Ref. [15], and the dash-dotted line describes the R_U-dependence of $\mathcal{M}_{\text{sum}\,F\,Mo}(R_U)$ (5.10). The dashed line displays the plutonium amount $\mathcal{M}_{n\,F\,Pu}(R_U)$ that stems within uranium sample due to the reaction (6.1)

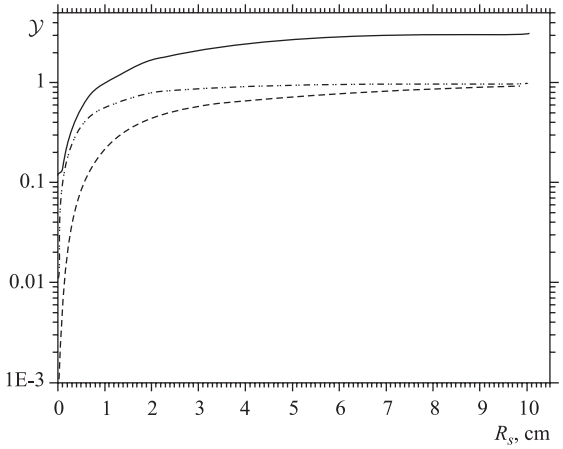

Fig. 5. The total activity $\mathcal{Y}$ (5.12) of ^{99}Mo and ^{239}Pu isotopes, produced within natural molybdenum and uranium samples, with the size R_S $(S = Mo, U)$ and area 1 cm^2, by the electron current with $\bar{E}_e = 50$ MeV and $J_e = 1$ A/cm^2, during 1 h. The solid line presents the R_{Mo}-dependence of the quantity $\mathcal{Y}_{\gamma\,Mo}(R_{Mo})[\text{kBq} \cdot 10^{10}]$, considered in Ref. [15], and the dash-dotted line describes the R_U-dependence of the quantity $\mathcal{Y}_{\text{sum}\,F\,Mo}(R_U)[\text{kBq} \cdot 10^{10}]$. The dashed line describes the R_U-dependence of total plutonium activity $\mathcal{Y}_{n\,F\,Pu}(R_U)[\text{kBq} \cdot 10^{3}]$ that stems within uranium sample due to the reaction (6.1)

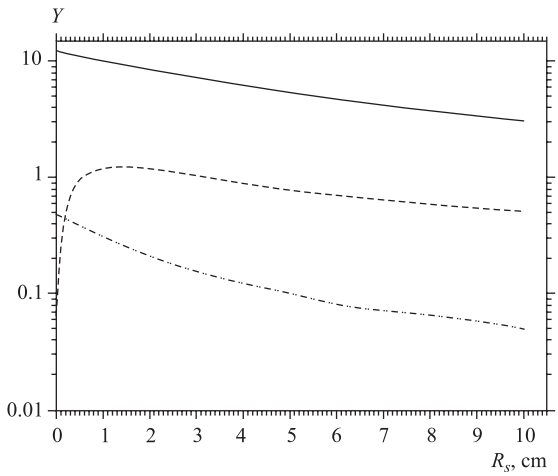

Fig. 6. The specific activity Y (5.11) of ^{99}Mo and ^{239}Pu, produced within natural molybdenum and uranium samples, with the size R_S $(S = Mo, U)$ and area 1 cm^2, by the electron current with $\bar{E}_e = 50$ MeV and $J_e = 1$ A/cm^2, during 1 h. The solid line presents the R_{Mo}-dependence of the quantity $Y_{\gamma\, Mo}(R_{Mo})\left[\dfrac{\text{kBq}}{\text{h}\cdot\boldsymbol{\mu}\text{A}\cdot\text{mg}^{100}\text{Mo}}\right]$, considered in Ref. [15], and the dash-dotted line describes the R_U-dependence of the quantity $Y_{\text{sum}\, F\, Mo}(R_U)\left[\dfrac{\text{kBq}}{\text{h}\cdot\boldsymbol{\mu}\text{A}\cdot\text{mg}^{238}\text{U}}\right]$. The dashed line describes the R_U-dependence of specific plutonium activity $Y_{n\, F\, Pu}(R_U)\left[\dfrac{\text{kBq}\cdot 10^{-8}}{\text{h}\cdot\boldsymbol{\mu}\text{A}\cdot\text{mg}^{238}\text{U}}\right]$ that stems within uranium sample due to the reaction (6.1)

On purpose to treat the practicable ^{99}Mo isotope production, we are also to acquire the dependence of ^{99}Mo yield through the uranium fission on exposition time T_e, alike this was done in obtaining with the photo-neutron reaction, see Ref. [15]. The dependence of the quantities $\mathcal{M}, \mathcal{Y}, Y$ on exposition time T_e is displayed in Figs. 7–9. Apparently, this dependence is substantially nonlinear at large enough $T_e \gtrsim 15$ h, in particular for the specific activity Y, see Fig. 9. There sees gradual saturation of the functions $\mathcal{M}_{(\gamma,n)\, F\, Mo}(T_e)$, $\mathcal{Y}_{(\gamma,n)\, F\, Mo}(T_e)$, and decrease of the specific activity $Y_{(\gamma,n)\, Mo}(T_e)$ with T_e growth.

The heretofore treated isotope ^{99}Mo is known to serve as a precursor giving rise to the most practicable meta-stable radio isotope ^{99m}Tc, with the lifetime $\tau_{^{99m}Tc} \approx 10$ h, that stems due to the ^{99}Mo β-decay

$$^{99}\text{Mo} \longrightarrow {}^{99m}\text{Tc} + e^-, \tag{5.13}$$

with the branching $\approx 85\%$. This reaction typifies a needful isotope generation via decay of a firstly obtained parent isotope. The ^{99m}Tc yield, accompanying the

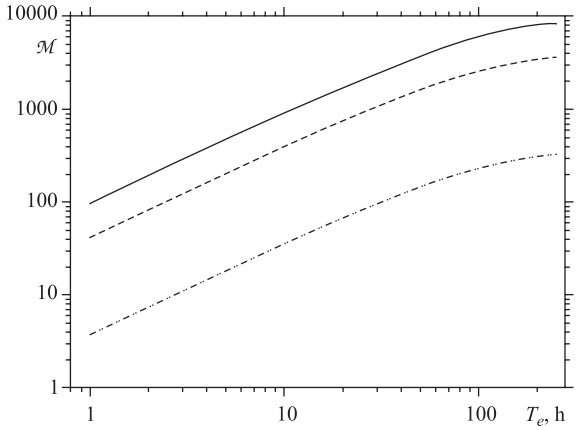

Fig. 7. The exposition time T_e[h]-dependence of the ^{99}Mo amount $\mathcal{M}(T_e)$[mg $\cdot$ 10^{-2}], produced within natural molybdenum and uranium samples, with the size $R_S = 2$ cm $(S = Mo, U)$ and area 1 cm^2, by the electron current with $\bar{E}_e = 50$ MeV and $J_e =$ 1 A/cm^2. The solid line describes the quantity $\mathcal{M}_{\gamma\, Mo}(T_e)$ considered in Ref. [15], whereas the dashed and dash-dotted lines stand for the determined by Eq. (5.10) quantities $\mathcal{M}_{\gamma\, F\, Mo}(T_e)$ and $\mathcal{M}_{n\, F\, Mo}(T_e)$, respectively

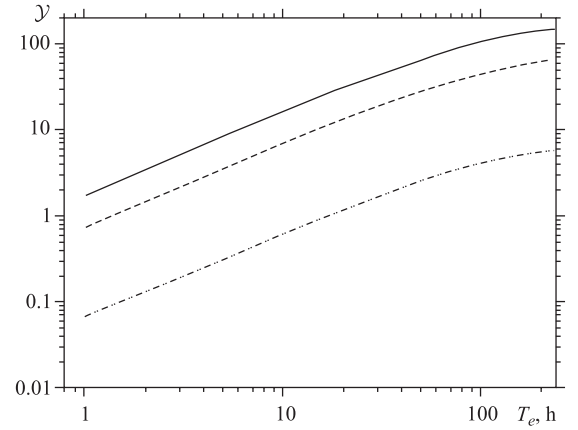

Fig. 8. The same as in Fig. 7, yet for the total activities: $\mathcal{Y}_{\gamma\, Mo}(T_e)$[kBq $\cdot$ 10^{10}] was considered in Ref. [15], solid line, whereas the dashed and dash-dotted lines stand for the determined by Eq. (5.12) quantities $\mathcal{Y}_{\gamma\, F\, Mo}(T_e)$ and $\mathcal{Y}_{n\, F\, Mo}(T_e)$, respectively

respective yield of ^{99}Mo, was thoroughly explored in the previous work [15], and those findings hold truth in the considered case as well, to all intents and purposes. Let us recall, the extreme ^{99m}Tc activity is accumulated in the irradiated sample

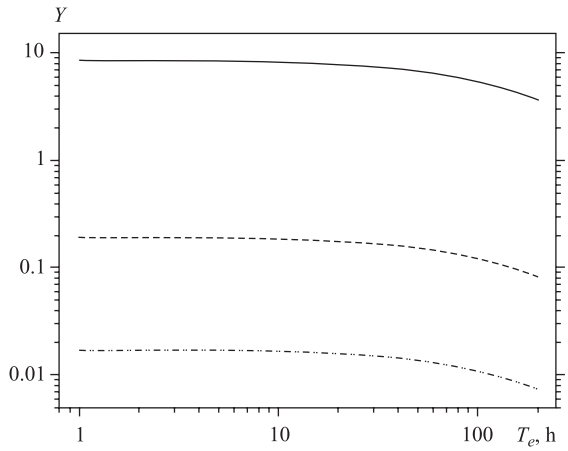

Fig. 9. The same as in Fig. 8, yet for the respective specific activities: $Y_{\gamma\,Mo}(T_e)\left[\dfrac{\text{kBq}}{\text{h}\cdot\boldsymbol{\mu}\text{A}\cdot\text{mg}^{100}\text{Mo}}\right]$, calculated in Ref. [15], and $Y_{\gamma\,F\,Mo}(T_e)\left[\dfrac{\text{kBq}}{\text{h}\cdot\boldsymbol{\mu}\text{A}\cdot\text{mg}^{238}\text{U}}\right]$ and $Y_{\gamma\,Mo}(T_e)\left[\dfrac{\text{kBq}}{\text{h}\cdot\boldsymbol{\mu}\text{A}\cdot\text{mg}^{238}\text{U}}\right]$, determined by Eq. (5.11)

in about 20 h after the end of exposition. Upon extracting this ^{99m}Tc amount, the next ^{99m}Tc portion, comparable with the first one, will again be accumulated in about 20 h, and so on.

6. THE NOXIOUS ISOTOPES EMERGENCE

Besides the just above-considered ^{238}U fission (4.14), the neutrons, produced in uranium sample by γ irradiating, are known to induce manifold other nuclear processes, which can result in emergence of some undesirable harmful stuffs. Among those, the reaction

$$n + {}^{238}\text{U} = \gamma + {}^{239}\text{U} \tag{6.1}$$

is understood to deserve a special concern. In fact, the ^{239}U radiative decay chain

$${}^{239}\text{U}^{(\beta^-)} \longrightarrow {}^{239}\text{Ne}^{(\beta^-)} \longrightarrow {}^{239}\text{Pu} \tag{6.2}$$

results in a short enough time $t \approx 3.4$ d, in the α-active radio isotope ^{239}Pu, with the lifetime [23, 24]

$$\tau_{^{239}Pu} \approx 35189 \text{ y} \ggg \tau_{^{99}Mo}. \tag{6.3}$$

Thus, side by side with the desirable ^{99}Mo production, we encounter the inescapable plutonium contamination of an uranium sample we deal with. Surely, plutonium is hot a sole toxicant substance accumulated inside irradiated ^{238}U sample, yet it is considered to be rather the most harmful one (see, e.g., Ref. [35]). The long lifetime (6.3) and the large enough energy $E_\alpha \approx 5$ MeV of emitted α-particles cause the especial biological harm of the contamination by ^{239}Pu isotope, so that a particular care should be taken to refine of the recovered ^{99}Mo from any minute amount of ^{239}Pu. To realize how dangerous the plutonium contamination can be, we are now to explore the ^{239}Pu yield due to the processes (6.1), (6.2), which accompanies inevitably the ^{99}Mo production in an uranium sample.

The total rate of ^{239}Pu production is directly determined by Eqs. (4.2), (4.4), (4.11), (4.13) with the tag $\mathbf{S} = \gamma$ and the cross section $\sigma_{n\mathbf{S}} = \sigma_{n\gamma} \sim 5$ b of the reaction (6.2) which is acquired from Ref. [34]. Despite a rather intricate form of the function $\sigma_{n\gamma}(\epsilon)$ [34], it proves to be consistently utilized in the evaluations we carried out. Let us note that each reaction (6.1) results in production of one ^{239}Pu nucleus, whereas the factor 0.06 in Eq. (5.1), describing the ^{99}Mo production in the ^{238}U fission by neutrons, allows for the ^{99}Mo share in the blend of ^{238}U fission fragments. Thus, the rate of ^{239}Pu production is just given by the expressions (3.25), (4.4), (4.11), (4.13) with $\mathbf{S} = \gamma$,

$$\frac{\mathrm{d}\mathcal{N}_{n\gamma\,Pu}(R_U, R_W, \bar{E}_e, t)}{\mathrm{d}t} = \frac{\mathrm{d}\mathcal{N}_{n\gamma}(R_U, R_W, \bar{E}_e, t)}{\mathrm{d}t}. \tag{6.4}$$

Consequently, the yield of ^{239}Pu amount $\mathcal{M}_{n\gamma\,Pu}(\mathrm{g})$, the total activity $\mathcal{Y}_{n\gamma\,Pu}(\mathrm{Bq})$ and the specific activity $Y_{n\gamma\,Pu}[\mathrm{Bq}/(\mathrm{h}\cdot\mu\mathrm{A}\cdot\mathrm{mg}^{238}\mathrm{U})]$ are evaluated according to Eqs. (5.10)–(5.12), with replacing therein $\mathcal{N}_{nF\,Mo}(R_U, R_W, \bar{E}_e, t)$ (5.1) by $\mathcal{N}_{n\gamma\,Pu}(R_U, R_W, \bar{E}_e, t)$, and $\tau_{^{99}\mathrm{Mo}}$ by $\tau_{^{239}\mathrm{Pu}}$ (6.3). The obtained results are presented in Table 4 and displayed by the dashed lines in Figs. 4–6. As seen, the produced ^{99}Mo amount $\mathcal{M}_{\mathrm{sum}\,F\,Mo}(R_U, R_W, \bar{E}_e, t)$ is anyway only twice as much as the $\mathcal{M}_{n\gamma\,Pu}(R_U,\, R_W,\, \bar{E}_e,\, t)$ worked up thereby. Of course, as the lifetime of ^{239}Pu (6.3) is rather not comparable with the ^{99}Mo one, the yield

Table 4. The yield of amount $\mathcal{M}$ and activities $Y, \mathcal{Y}$ of ^{239}Pu originated due to the reaction ^{238}U$(n,\gamma)^{239}$U induced by the neutrons that stem within an ^{328}U sample, with $R_U = 2$ cm and 1 cm^2 area, due to the electron current with $\bar{E}_e$[MeV] and $J_e = 1$ A/cm^2, during 1 h

$\bar{E}_e$ [MeV]	20.0	25.0	50.0	100.0
$\mathcal{M}$ $[\mathrm{mg}\cdot 10^{-2}]$	3.36	6.51	19.43	34.34
Y $\left[\dfrac{\mathrm{kBq}\cdot 10^{-8}}{\mathrm{h}\cdot\mu\mathrm{A}\cdot\mathrm{mgU}}\right]$	0.20	0.40	1.20	0.09
$\mathcal{Y}$ [kBq]	76.24	147.7	441.0	779.6

of activities $\mathcal{Y}_{n\gamma\,Pu}$ and $Y_{n\gamma\,Pu}$ shows up to be negligible as compared to the respective activities of the ^{99}Mo simultaneously produced. Actually, yield of the noxious isotope ^{239}Pu is simply proportional to exposition time T_e, the life-time (6.3) being as long as it is. Such a need to dispose of the radio nuclei, in particular plutonium, contamination is certain to be substantial shortcoming of the ^{238}U-fission method as compared to the photo-neutron method of ^{99}Mo production [15].

7. SUMMARY

In conclusion, we brief anew the long and hard way that runs from the preparation of the sample to be irradiated towards the end-consumers of radio isotopes. In comparing and confronting at every stage the different timely practicable methods of radio isotopes production, we are to elucidate all the advantages and shortcomings of them.

There is no deal of work to make a ^{238}U target in the case considered in the work presented. For the photo-neutron production method, the irradiated sample is to be properly wrought up to incorporate as much as feasible the very isotope which serves to produce the desirable radio isotope. In particular, for the marketable ^{99}Mo isotope yield [15], the natural molybdenum $^{\rm nat}$Mo is to be enriched so as an irradiated sample would consist of pure ^{100}Mo isotope, which is today known to be well practicable [36]. Far more complicated and work-consuming is the target preparation for the routine isotope production through the ^{235}U fission by neutrons in the research and test reactors [2, 7], no matter whether the highly-enriched-uranium (HEU) or low-enriched-uranium (LEU) target is utilized.

There is no trouble in placing (as well as replacing) a sample for exposition by the γ-flux converted from electron beam of an accelerator, in particular as the electron accelerator can be turned on and off at will and without consequence. On the very contrary, it is a great deal of sophisticated work to manage the appropriate irradiation of an uranium sample (on matter HEU or LEU is utilized) inside active zone of a high-flux reactor.

There is actually no issue in cooling the tungsten electron$-\gamma$-ray converter and the irradiated sample, which is a point in favor of the e-linac-driven production method as well. Let us recall, there sees no need of the sample size $R_{Mo,\,U}$ being greater than ~ 2 cm, for marketable radio isotope manufacture.

Operating expenditures themselves of an e-linac should also be far lower than ones of a new-build specially dedicated reactor, as much less staff and safety-related issues are involved. All the more so, when we deal with an aging obsolescent reactor, for now being used. In addition, at any malfunction, to refurbish the e-linac and bring it online is far easier than the high-flux reactor.

The key point at issue is productivity of different methods to produce various isotopes, in particular the most extensively employed medical radio isotope ^{99}Mo. According to the data presented in Table 3 and in Fig. 8, the total molybdenum activity $\mathcal{Y}_{\mathrm{sum}FMo}$ generated in a practicable uranium sample with the length $R_U = 2$ cm and the 1 cm^2 area, due to the electron beam with $\bar{E}_e = 50$ MeV and a given current $J_e \left[\dfrac{\mathrm{A}}{\mathrm{cm}^2}\right]$, during an exposition time T_e[h], is found to be

$$\mathcal{Y}_{\mathrm{sum}FMo}(T_e, J_e) \approx 0.08 \cdot J_e \cdot T_e \cdot 10^{11}\mathrm{kBq} \approx 0.25 \cdot J_e \cdot T_e \cdot 10^3\mathrm{Ci}, \qquad (7.1)$$

pursuing the method explicated in the work presented. In the previous work [15], the respective yield of total activity $\mathcal{Y}_{^{99}Mo}$ in the photo-neutron reaction $^{100}\mathrm{Mo}(\gamma, n)^{99}\mathrm{Mo}$ was found to be

$$\mathcal{Y}_{^{99}\mathrm{Mo}}(T_e, J_e, \mathcal{A}_{bn}) \approx J_e \cdot T_e \cdot \mathcal{A}_{bn} \cdot 1.7 \cdot 10^{11}\mathrm{kBq} \approx 5 \cdot 10^3 \cdot J_e \cdot T_e \cdot \mathcal{A}_{bn}\mathrm{Ci}, \quad (7.2)$$

the irradiated Mo sample having the same length $R_{Mo} = 2$ cm and 1 cm^2 area. The factor $\mathcal{A}_{bn}$ allows for the ^{100}Mo isotope share in the sample; for natural molybdenum $\mathcal{A}_{bn} \approx 0.1$. As understood, either avenues lead to comparable issues when natural molybdenum sample, i.e., $\mathcal{A}_{bn} \approx 0.1$, is utilized in the ^{99}Mo photo-neutron production. Yet provided the irradiated molybdenum sample consists of pure ^{100}Mo isotope, the photo-neutron yield (7.2) favors apparently over the yield (7.1) through the ^{238}U fission. In the previous work [15], the accelerator-driven photo-neutron ^{99}Mo production was understood to be well competentive with the routine reactor-based production [1, 2, 7], so far a pure ^{100}Mo isotope sample is irradiated. The total weekly yield of activity would amount up to the value

$$\mathcal{Y}_{^{99}Mo} \approx 7.5 \cdot 10^3\mathrm{Ci}, \qquad (7.3)$$

the electron current having the reasonable value $J_e = 10\ \dfrac{\mathrm{mA}}{\mathrm{cm}^2}$ [3, 8].

Upon exposing, the irradiated sample has to be wrought over in order to recover the desirable isotope. For now, in the routine reactor-based isotope production method, there are applied the very special and costly *hot sells facilities* [7] to extract the ^{99}Mo medical isotope out of the blend of ^{235}U fission fragments and then purify it. This process lasts for days, it is very complicated, and must be carried out with the highest care and precaution, no matter, HEU or LEU targets are used. In fact, the akin operations are to be performed to recover the ^{99}Mo isotope out of the blend of fragments of the ^{238}U fission by γ-rays and neutrons, which is described in the presented work. Even though the aforesaid *hot sells facilities* can be thought to be adjusted somehow to this case, they are anyway to be tailored for the new task. Especially, a great deal of efforts has to be aimed towards disposing of the harmful isotope ^{329}Pu, emerging inevitably in the ^{99}Mo production through ^{238}U fission, as explored in Sec. 6.

On the contrary, in the photo-neutron production, as considered in Ref. [15], the desired isotope ^{99}Mo is obtained within a pure molybdenum target, so that we are not in need of any *hot sells facilities*. There is no need to purify anything and manage any wastes, as a matter of fact, though the appropriate ancillary equipment is to be designed anew. There emerge no noxious admixtures and impurities in irradiated sample to be disposed of them, as, for instance, the ^{239}Pu isotope, see Sec. 6. Consequently, the recovered ^{99}Mo shipment to market is practically feasible just after the end of exposition, without any palpable delay. Therefore, the six-day term, *6-day curies* [1, 2, 7], for calibrating the activity of output can be recounted just from the end of exposition. As ^{99}Mo lifetime $\tau_{^{99}Mo} \approx 96$ h, the *weekly 6-day curies activity* corresponding to (7.3) results as

$$\mathcal{Y}_{\textit{6-day}} \approx 1.67 \cdot 10^3 \text{Ci}, \tag{7.4}$$

which is competitive with the *large-scale* productivity of the *large-scale producer* who supplies more than 1000 *6-day curies per week* to the market, on the routine reactor bases, with operating the HEU targets.

There is no issue of shipment of ^{99}Mo to the facilities manufacturing the ^{99m}*Tc generators* [3, 7, 8], which must be anew designed and adjusted to handle irradiated molybdenum samples in the photo-neutron production method. The losses of radio-isotope yield caused by decay rate would be in this case minimized, and even almost eliminated, by co-locating all the engaged facilities. Under such circumstances, any irradiated ^{100}Mo target, upon utilizing by *Tc-generator*, would be restored, and then exposed anew. A circle of this kind could many times be repeated which would allow saving the stick of starting enriched material, e.g., the ^{100}Mo isotope, in producing the ^{99}Mo isotope. That agenda would offer the possibility of self-contained generator systems being feasible for central radio-pharmaceutical labs for a group of hospitals. So, for all we have acquired, there offers a new stream from the ^{99}Mo production to an end-user consumption of *kits* prepared with ^{99m}Tc.

We must although keep in view that both the routine ^{325}U fission in high-flux reactors and the e-linac-driven ^{238}U fission, treated in the work presented, can serve to produce only the nuclei with $A \approx 100$ and $A \approx 140$ [23–25], whereas the photo-neutron method elaborated in Refs. [11–15] is eligible to produce immense variety of radio isotopes, in particular such as ^{13}N, ^{18}F, ^{45}Ti, underlying the timely rapidly developing *positron emission tomography, PET*.

At last, not only the cost of an e-linac is far lower than that of a timely dedicated reactor, but decommissioning an e-linac is also extremely less expensive than that of a reactor.

Acknowledgements. Authors are grateful to Z. Panteleev, Yu. P. Gangrsky for the valuable discussions.

REFERENCES

1. Isotope Production and Application in the 21st Century // Proc. of the Third Intern. Conference on Isotopes, Vancouver, Canada, 6–10 September, 1999. World Sci. Pub. Co. In. Vancouver, B. C. Stevenson, 2000.
2. Isotopes for Medicine and Life Science. Committee on Biomedical Isotopes / Ed. S. J. Adelstein, F. J. Manning. Washington D.C.: National Academies Press, 1999.
3. Isotope Production and Applications. Workshop on the Nation's Needs for Isotopes: Present and Future. Rockwille, MD, August 5–7 2008. U.S. Depatament of Energy, 2008.
4. *Troger G. L., Schenter R. E.* // J. Radioanal. Nucl. Chem. 2009. V. 282. P. 243.
5. *Enstein A. J.* // J. Am. Coll. Cardiol. Img. 2009. V. 2. P. 369.
6. *Ruth T.* // Nature. 2009. V. 457. P. 536;
   Ruth T. // Rep. Prog. Phys. 2009. V. 72. P. 016701.
7. Medical Isotope Production without Highly Enriched Uranium. National Research Council of the National Academies, C. G. Whippl (chair). The National Academies Press, Washington D.C., 2009.
8. Making Medical Isotopes. Report of the Task Force on Alternatives for Medical-Isotope Production / Ed. A. Fong, T. I. Meyer, K. Zala. AAPS, Canada, TRIUMF, 2008.
9. *Henning W. et al.* Radioisotope for Science and Medicine. Accelerators for America's Future Symposium. Washington DC, Oct. 2009.
10. *Bertsche K.* Accelerator Production Options for ^{99}Mo // Proc. of IPAC'10, Kyoto, Japan, May 2010. P. 121.
11. *Sabel'nikov A. B. et al.* // Radiochemistry. 2006. V. 48. P. 191.
12. *Sabel'nikov A. B. et al.* // Ibid. P. 187.
13. *Dmitriev S. N. et al.* // Radiochemistry. 1998. V. 40. P. 552.
14. *Dmitriev S. N., Zaitzeva N. G.* // Radiochemica Acta. 2005. V. 93. P. 571.
15. *Bunatian G. G., Nikolenko V. G., Popov A. B.* JINR Commun. E-2009-182. Dubna, 2009.
16. Landolt-Börnstein. Elementary Particles, Nuclei and Atoms, 16 A / Ed. H. Shopper, Springer, 2000.
17. *Veyssiere A. et al.* // Nucl. Phys. A. 1973. V. 199. P. 45;
    Caldwel J. T., Dowdy E. J., Berman B. L. // Phys. Rev. C. 1980. V. 21. P. 1215.
18. *Akhiezer A. I., Berestetskii V. B.* Quantum Electrodynamics. M.: FM, 1959.
19. *Heitler W.* The Quantum Theory of Radiation. Oxford, London: Clarendon Press, 1954.
20. *Berestetskii V. B., Lifshits E. M., Pitaevskii L. P.* Relativistic Quantum Theory. Oxford: Pergamon, 1971.
21. *Shiff L. I.* // Phis. Rev. 1951. V. 83. P. 252.
22. *Bethe H., Heitler W.* // Proc. Roy. Soc. A. 1934. V. 146. P. 83.
23. The Nuclear Handbook / Ed. O. R. Frisch. London: George Newnes Limited, 1958;
    The Tables of Physical Quantities / Ed. I. K. Kikoin. M.: Atomizdat, 1976.

24. *Katcoff S.* // Nucleonics. 1960. V. 18. P. 201;
Ziskin Yu. A., Lbov A. A., Sel'genkov L. I. Fission Products and Their Mass Distributions. M.: Gosatomizdat, 1963;
Gangrsky Yu. P., Markov B. N., Pereligin V. P. Fission Fragments Registration and Spectrometry. M.: Energoatomizdat, 1992.
25. The Nucl. Fis. Proc. / Ed. C. Wagemans, CRC Press, BOCA, Rafon, 1991.
26. *Veyssiere A. et al.* // Nucl. Phys. A. 1968. V. 121. P. 463;
Veyssiere A. et al. // Nucl. Phys. A. 1970. V. 159. P. 561.
27. *Blatt J. M., Weisskopf V. F.* Theoretical Nuclear Physics. New-York-London, 1952;
Berman B. L., Fultz S. C. // Rev. Mod. Phys. 1975. V. 47. P. 739.
28. *Barret R. F. et al.* // Nucl. Phys. A. 1973. V. 210. P. 355.
29. *Lui J. C. et al.* // Rad. Prot. Dosimetry. 1997. V. 70, No. 1–4. P. 49. (Nucl. Thech. Pub.).
30. *Poenitz W. P. et al.* // Argone Nat. Lab. Rep. ANL-NDM-80, 1983;
Hayes S. et al. // Nucl. Sci. Eng. 1973. V. 50. P. 243;
Tsubone I. et al. // Nucl. Sci. Eng. 1984. V. 88. P. 579.
31. *Poenitz W. P., Fawcett L. R., Smith D. L.* // Nucl. Sci. Eng. 1981. V. 78. P. 239.
32. *Frohner F. H.* // Nucl. Sci. Eng. 1988. V. 103. P. 251.
33. *Kawano T. et al.* JAERI-Research (2000) 2000-004.
34. *McDaniels D. K. et al.* // Nucl. Phys. A. 1982. V. 384. P. 88;
Darke D., Bergqwist M. I., McDaniels D. K. // Phys. Lett. B. 1971. V. 36. P. 557.
35. Draft Toxicological Profile for Plutonium. Agency for Toxic Substances and Disease Registry / Ed. H. Frumkin, J. L. Gerberding, Atlanta, Georgia, Sep. 2007.
36. *Bekman I. N.* Radioactivity and Radiation (Lecture 7). Moscow State University, Moscow, 2006;
Bigelow T. S. et al. Production of Stable Isotopes Utilizing the Plasma Separation Process. WILEY, Inter Science, 2005.
Matthews M. D. Systems and Methods for Isotope Separation. Pub. No.: U.S. 2007/0272557 A1, Nov. 29, 2007.

Received on July 21, 2010.

Редактор *В. В. Булатова*

Подписано в печать 07.10.2010.
Формат 60 × 90/16. Бумага офсетная. Печать офсетная.
Усл. печ. л. 2,06. Уч.-изд. л. 2,84. Тираж 290 экз. Заказ № 57110.

Издательский отдел Объединенного института ядерных исследований
141980, г. Дубна, Московская обл., ул. Жолио-Кюри, 6.
E-mail: publish@jinr.ru
www.jinr.ru/publish/